Tight-binding study of hydrogen on the C(111), C(100), and C(110) diamond surfaces

B. N. Davidson and W. E. Pickett
Complex Systems Theory Branch, Naval Research Laboratory, Washington, D.C. 20375-5345
(Received 24 September 1993)

The band structure, total energies, and relaxed geometries are calculated for the C(111), C(100), and C(110) surfaces using a parametrized tight-binding model for carbon. The method and addition of C-H parameters to the model are described in detail. Results for the bare and hydrogenated C(111) surfaces are used to compare the accuracy of the method with *ab initio* techniques. A stable hydrogenated (2×1) π reconstructed surface is found, which resembles the C(110) surface. Removal of one H atom from the dihydride C(100) results in a $\frac{3}{2}$ hydride surface, where the odd hydrogen is bonded equally to two surface carbons. Although the fully H-covered C(100)(2×1) surface has a clean gap, the partially covered surface has a half-filled state, consistent with photoemission data. The geometries and H vibrations are also presented for the C(110) surface. The surface chains on the bare C(110) have bond lengths close to graphite and dimerize from a Peierls distortion. Addition of H to this surface restores the bond lengths to approximately that of bulk diamond. Comparison of the band structures and H vibrations with experiment helps identify the nature of the hydrogen coverage on the surfaces.

I. INTRODUCTION

Diamond thin films can be grown under conditions of low pressure with the chemical vapor deposition (CVD) of an excited hydrocarbon gas. Mechanisms have been proposed that include the attachment of hydrocarbons to the C(111), C(100), and C(110) surfaces to describe the CVD growth of diamond films.[1] There is much disagreement in these models regarding which hydrocarbon molecules are predominantly responsible for diamond growth. Though much attention has been paid to the gas phase chemistry above the substrate, in attempts to identify the molecules in the gas, more still needs to be learned about the precise nature of the surface to understand how these hydrocarbons can bond.

Unlike other group-IV elements that prefer an sp^3 bonded diamond structure, such as Si and Ge, C is unique in that it also forms a competing sp^2 bonded graphite phase. At atmospheric conditions, the graphite phase is the most stable, and one would expect sp^2 bonded growth under the conditions typical of CVD. Instead, the structure of the substrate surface promotes sp^3 bonding in a wide variety of conditions. Experimental studies have been performed to probe all three high-index C surfaces in order to determine the structure of the surface. Lurie and Wilson[2] examined the C(111), C(100), and C(110) surfaces with low-energy electron diffraction (LEED) and found (1×1) patterns for all three surfaces, and (2×1) patterns for the C(100) and C(111) surfaces at elevated temperatures above $\sim 1000\,^{\circ}$C. For the C(111), Pate[3] showed that the graphite surface layer would also exhibit the same (1×1) pattern, but with a slightly mismatched lattice constant. This mismatch would produce rings or rotated (1×1) patterns, which he did not find and therefore concluded that the (1×1) symmetry resembled the bulklike diamond configuration. Pate also pointed out that a graphite layer could not yield the (2×1) LEED pattern that was observed, indicating that the reconstructed surface was some structure other than a graphite layer.

A H atmosphere above the substrate promotes sp^3 bonding during film growth and substantially increases the quality of the diamond, but it still remains unclear how this happens. One view is that H preferentially etches graphite over diamond, thereby promoting sp^3 bonding, but it has also been observed that H can also aid in preventing (2×1) reconstruction of the surfaces. Photon-stimulated ion desorption (PSID)[4] and vibration studies using high-resolution electron-energy loss (EEL)[5] have determined that the C(111) (1×1) surface is H terminated, and that the reconstructed surface is relatively H free, but still reactive to atomic H. Electron-stimulated desorption time-of-flight (ESD-TOF) experiments found that the desorption of H from the C(111) surface precedes reconstruction[6] and more recently it was reported that dosing a (2×1) surface with H initiates reconstruction back to a (1×1) surface.[7] Similar studies on the C(100)[8] and C(110)[9] (1×1) surfaces found that these were also covered with H. In the case of the C(100) surface, two distinct H bonds were identified with ESD-TOF experiments.[8]

Photoemission experiments on the C(111),[4,10] C(100),[8] and C(110)[9] planes find that the (1×1) surfaces have no states in the gap. *Ab initio* calculations on the C(111) surface have been performed indicating that the bare C(111) surface should have both occupied and unoccupied states in the gap.[11–13] Since H is believed to remove gap states, this confirms the conclusion that the (1×1) C(111) surface is fully H covered. The extent of the H coverage for the (2×1) surfaces at elevated temperatures still remains unclear. Hamza *et al.*[8] reported that H was still bonded to the (2×1) C(100) surface,

0163-1829/94/49(16)/11253(15)/$06.00

in the gap, but *ab initio* calculations have found that the (2 × 1) H-terminated surface should have no states in the gap[14]. EEL data has also indicated that band-gap states appear when the C(110) surface is heated above ~ 900 °C,[9] but as far as we know, there have been no published total-energy calculations on the C(110) surfaces.

Ab initio methods are probably the most accurate methods for resolving some of these issues concerning the diamond surface, but are limited by their demand for computational time and/or memory. To overcome these limitations, empirical and semiempirical total-energy methods have been adopted for the study of the diamond surface. A detailed potential to accurately model hydrocarbons and diamond surfaces was developed by Brenner[15] and was used for predicting the energetics of H abstraction from the C(111) and C(100) surfaces and for performing very large-scale simulations involving diamond surfaces.[16] One drawback of applying a classical potential is that the electronic states on the surface are not explicitly considered, so that these methods cannot be used to investigate the gap states or any surface behavior driven by changes in the electronic band structure. Semiempirical methods have been adopted so that the electronic energy could be explicitly included in the calculation of the total energy. Modified neglect of differential overlap (MNDO) methods have been applied to clusters that resemble the diamond surfaces.[17] Bechstedt and Reichardt used a tight-binding method to minimize the energy and determine the structure of the C(111) surface,[18] but their band structure energy was modeled as a sum over nearest-neighbor, parametrized bond energies so the band structure was not calculated. Zheng and Smith have used a slab-MNDO method to study the C(111) (Ref. 19) and C(100) (Ref. 20) hydrogenated surfaces. Unlike typical MNDO calculations, their parameters were fitted to bulk properties rather than molecular values, but they limited the size of their slabs to approximately the same number of layers as the more accurate *ab initio* studies so the advantage of their empirical method is not clear.

In this paper, we describe a parametrized tight-binding energy functional (PTBF) method that has been optimized to yield accurate total energies over a range of bond distances and lattice constants for C.[21] Since the role of H is important to diamond growth, we add parameters for the C-H bond to this model. The advantage of using this PTBF approach is that the band structure, relaxed total energies, and vibrations on the surface can be calculated relatively quickly on a workstation, which allows for the examination of larger systems than those used in previous calculations without a substantial loss of accuracy. This approach is not meant to be a substitution for *ab initio* methods, such as density functional (DF) theory, but rather a complementary technique for understanding the surface behavior, provide starting configurations, or determine the number of atoms and/or $\vec{k}$ points that are needed to correctly perform an *ab initio* calculation. The purpose of this paper is twofold: (1) to describe the method and the parameters and (2) to apply the PTBF method to the hydrogenated C(111), C(100), and C(110) surfaces, examining the total energies, relaxed geometries, band structure, and vibration modes on the surfaces.

II. TIGHT-BINDING METHOD

The PTBF method uses a parametrized Hamiltonian to obtain the electronic energy levels of a molecule or solid. The matrix elements of the Hamiltonian can be approximated with two-center integrals between atomic-like basis functions centered on each atom. By treating these integrals as adjustable parameters, they can be found from a fit to the electronic states at a small number of $\vec{k}$ points.[23] Once a proper fit is found, the band structure at all $\vec{k}$ points can be calculated. In addition, the TB band structure does not inherently suffer from an inadequacy to produce correct band gaps as does DF theory. These parameters have been obtained for many materials[24,25] and provide a reliable and fast method for calculating band structure energies. The total energy of a molecule or solid can be written within the PTBF framework as:

$$E_{\rm tot} = E_{\rm bs} + E_{\rm rep} \tag{1}$$

where $E_{\rm bs}$ is the sum of the occupied electronic states and $E_{\rm rep}$ incorporates all other repulsive energies. Chadi[26] has successfully used this approach to study the surface geometries of GaAs, ZnSe, and Si by fitting his repulsive term to the lattice constant and bulk modulus. A more comprehensive PTBF form for the total energy, suggested by Tománek and Schlüter,[27] was used for calculating the stability and structure of small clusters and included a Hubbard-like charge term which increased the energy of the molecule when there was excess localized charge.

A critical issue for using a PTBF approach is the problem of the transferability of the parameters as lattice constants or chemical environments are changed. Harrison has suggested a universal d^{-2} distance scaling law of the two-center parameters for s- and p-like orbitals.[25] This approximation can be very useful, especially near the equilibrium bond length, or when trying to approximate parameters of chemically similar materials with slightly different lattice constants, but it is not very accurate far away from the equilibrium bond lengths. Allen *et al.*[28] handled this problem by simultaneously fitting the two-center parameters of a nonorthogonal sp^3 basis to the band structures of solid Si with different lattice constants and then fitting these parameters to a polynomial function of distance. Suggestive of two-center terms in DF theory, Goodwin *et al.*[29] proposed a functional form for scaling both the electronic parameters and the pairwise repulsive term,

$$h(r) = h_0 \left(\frac{r_0}{r}\right)^n \exp\left[n\left(\left(\frac{r_0}{r_c}\right)^m - \left(\frac{r}{r_c}\right)^m\right)\right], \tag{2}$$

and were able to reproduce the total energies of Si in different phases.[29]

By following the approach of Goodwin *et al.*, Xu *et al.*[21] obtained a set of parameters, fitted simultaneously

to the total energies (calculated by DF theory) of three phases of C: an infinite linear chain, graphite, and diamond. Unlike Goodwin *et al.*'s approach, two distinct functions, of the same form as $h(r)$, were used to scale the electronic parameters $s(r)$ and model the pairwise repulsive potential $\phi(r)$:

$$s(r) = \left(\frac{r_0}{r}\right)^n \exp\left[n\left(\left(\frac{r_0}{r_c}\right)^{n_c} - \left(\frac{r}{r_c}\right)^{n_c}\right)\right], \quad (3)$$

$$\phi(r) = \phi_0 \left(\frac{d_0}{r}\right)^m \exp\left[m\left(\left(\frac{d_0}{d_c}\right)^{m_c} - \left(\frac{r}{d_c}\right)^{m_c}\right)\right]. \quad (4)$$

Rather than a simple sum over ion pairs, the repulsive energy is written as an adjustable fourth-order polynomial function of $\phi(r)$ to incorporate higher-order terms in r_{ij},

$$E_{\text{rep}} = \sum_i f\left(\sum_j \phi(r_{ij})\right). \quad (5)$$

The functions $s(r)$ and $\phi(r)$ are smoothly cut off at approximately 2.6 Å, the second-neighbor distance in bulk diamond, by the addition of a third-order polynomial tail. The coefficients of this polynomial are uniquely determined by the conditions that the functions $s(r)$ and $\phi(r)$ and their first derivatives go continuously to zero at the cutoff. All of the parameters in Eqs. (3), (4), and (5) together with the electronic two-center integrals of an sp^3 basis were used in fitting to the total energy over a range of lattice constants from ~ 1.2 to ~ 1.7 Å for all three phases of C. The resulting parameters of this fit are listed in Ref. 21, which also gives the calculated phonon frequencies, bulk modulus, and Grüneisen parameters for diamond and graphite. For finite or semifinite systems such as clusters and surfaces, charge transfer is modeled by the addition of a Hubbard-like term,

$$H_u = \frac{1}{2}U \sum_i^{\text{atoms}} \left(q_i - q_i^0\right)^2 \quad (6)$$

where $U = 4$ eV, q_i^0 is the number of valence electrons contributed by the ith atom, and q_i is the Mulliken charge population at each atom.[30] This PTBF model has also been applied to simulations of amorphous C,[31] clusters,[21] and fullerenes.[22]

We obtained the additional TB parameters for C-H interactions from a fit to the electronic levels and energies of methane. A similar approach has been used previously for H on both Si (from a fit to silane),[32–34] C surfaces,[35,36] and C clusters.[37] These studies only considered the equilibrium C-H distance of the molecule. At equilibrium, the H bond length on a surface should not be much different from its value in a molecule, but in order to study a wider range of dynamics of the H atom on the surface, a simple scaling law for the H bond is not appropriate and a more robust set of parameters fit over a *range* of C-H bond lengths is required. We employ the all-electron, density functional code of Pederson and Jackson[38] to generate a database of accurate electronic levels, total energies, and forces for a methane molecule with variable bond lengths.

Rather than simultaneously fitting all the parameters to reproduce the total energies of methane, we first fit just the two-center electronic parameters and scaling function to the occupied eigenvalues of the molecule over a range of C-H bond lengths from 0.8 to 1.6 Å. The antibonding states do not contribute to the total energy of the molecule or the diamond surface, and by considering only the occupied levels we are able to get a very accurate fit. Each H atom contributes an s orbital to the molecule. By taking linear combinations of the four H s orbitals, the electronic levels separate into a singlet and a threefold state corresponding to H s interactions with the C s and p orbitals respectively. In terms of the two-center parameters, the eigenvalues of these states are written as

$$a_1 = \tfrac{1}{2}(E_{\text{H}} + E_s) - \left[(E_{\text{H}} - E_s)^2 + 16[s(r)V_{ss\sigma}]^2\right]^{\frac{1}{2}}, \quad (7)$$

$$t_2 = \tfrac{1}{2}(E_{\text{H}} + E_p) - \left[(E_{\text{H}} - E_p)^2 + \tfrac{16}{3}[s(r)V_{sp\sigma}]^2\right]^{\frac{1}{2}}, \quad (8)$$

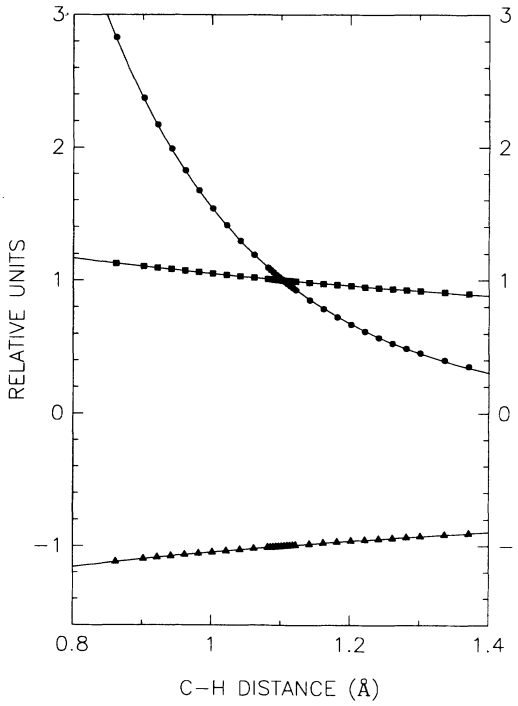

FIG. 1. Plot comparing the fit of the PTBF parameters (solid lines) with the electronic levels and forces of methane calculated by DF theory. Circles are the contribution of the repulsive term to the radial force. Triangles and squares are the sum and difference of the a_1 and t_2 electronic levels. The y axes of the plot have been normalized by their absolute values at the equilibrium bond length (~ 1.1 Å) of 10.66 eV/Å^2, 26.37 eV, and 7.48 eV for the repulsive force, sum, and difference of electronic levels, respectively.

TABLE I. C-H electronic tight-binding parameters from the fit to methane. The scaling function refers to Eq. (3) in the text. The value of r_0 is taken as the equilibrium bond length of methane, where the scaling function equals unity. The polynomial tail ensures that the parameters and their first derivatives go smoothly to zero between r_1 and $r_{\rm cut}$.

Two-center parameters (eV)					
$E_s^{\rm H}$	$V_{ss\sigma}^{\rm H\text{-}C}$	$V_{sp\sigma}^{\rm H\text{-}C}$	$V_{ss\sigma}^{\rm H\text{-}H}$	$E_s^{\rm C}$	$E_p^{\rm C}$
−4.74946	−6.52263	6.81127	0.00	−2.990	3.710
Parameters for scaling function					
n	n_c	r_0	r_c	r_1	$r_{\rm cut}$
0.234238	0.434526	1.10168	0.0522159	1.55	1.85
Polynomial tail $t_s(r-r_1)$					
	c_0	c_1	c_2	c_3	
	0.80179629	−0.35091957	−24.38707907	55.49321117	

where $s(r)$ is the scaling function appearing in Eq. (3). We chose to ignore the H-H interactions in these equations, since they should be small. We use the same on-site energies, E_s and E_p, for C as Xu *et al.*[21] so our fit would be consistent with their C parameters. Rather than fitting Eqs. (7) and (8) separately, we fitted to linear combinations $a_1 \pm t_2$ as a function of C-H distance. The resulting electronic parameters are listed in Table I and a comparison of our fit with the DF data is shown in Fig. 1. The two top curves in Fig. 1 are the sum and difference between the a_1 and t_2 levels. For convenience, the curves have been normalized by the value at the equilibrium C-H bond length of 1.1 Å.

The parameters in $E_{\rm rep}$ appearing in Eqs. (4) and (5) were fit to the forces $dE_{\rm tot}/dr_{\rm C\text{-}H}$ rather than the energies, for a better description of the dynamics of the C-H bond. Using the parameters in Table I, we calculate the force due to both the band structure term and the Hubbard-like charge term. These results are subtracted from the total force determined by the DF code, providing a data set for determining the adjustable parameters in $dE_{\rm rep}/dr_{\rm C\text{-}H}$. The coefficients of the fourth-order polynomial in Eq. (5) had to have the same values as used by Xu *et al.*, since it is a function of the sum over all the pairwise $\phi(r)$ which can include both C-C and C-H interactions. A comparison of the resulting fit to the DF data is shown in Fig. 1 and the parameters are listed in Table II. The lowest curve is a plot of $dE_{\rm rep}/dr_{\rm C-H}$, which has been normalized by its value at the equilibrium bond length. As a test of our forces, we calculated the vibrations of a CH_4 molecule. The f_2 and a_1 stretching modes are at 3093 and 2931 $\rm cm^{-1}$ compared with 3020 and 2914 $\rm cm^{-1}$ for experiment, respectively.[39] The e and f_2 bending modes are at 1631 and 1597 $\rm cm^{-1}$, compared with the experimental values of 1526 and 1306 $\rm cm^{-1}$.[39] Despite the fortuitously small error ($\sim 7\%$) in the e mode, the f_2 bending mode is not accurate because the parameters were fitted to the stretching rather than bending of the bond. Note that unlike the C parameters, the H parameters for the total energy are valid only with the use of the Hubbard term, since it was explicitly included in the forces.

For the case of the C(100) (1×1) surface, the H atoms bonded to the surface can be in close proximity to each other. In order to consider the hydrogenated C(100) surface, it is necessary to include the interaction between H atoms bonded to different C atoms (-H:H-) in the PTBF Hamiltonian. To model an environment similar to the C(100) surface, we brought two CH_4 molecules together with a C-H bond of each molecule along an axis. The other three C-H bonds were in a staggered, dihedral configuration to maximize the distance between them. By bringing the two molecules together, the degeneracy of the electronic states is partially broken so that we were able to fit the -H:H- parameters to the splitting of the methane levels over a -H:H- separation ranging from 0.6 to 1.1 Å. The repulsive terms were then calculated from the forces by following the same prescription as we did for the C-H bond, explicitly including the Hubbard term. These parameters are listed in Tables III and IV. It should be emphasized that these parameters are only valid for the interaction between two H atoms bonded to different C atoms and that they cannot be applied to any other H environment.

III. RESULTS AND DISCUSSION

All the surfaces are modeled with supercells of atoms, periodic in two dimensions. Each slab has inversion symmetry about a point in the center of the cell. The number of layers are chosen so that the forces and the elec-

TABLE II. Repulsive parameters for the C-H bond. These parameters refer to Eq. (4). See text for full details.

Parameters for $\phi(r)$						
ϕ_0	m	m_c	d_0	d_c	d_1	$d_{\rm cut}$
9.1175	0.709795	0.867909	0.785648	0.1400	1.605	1.85
Polynomial tail $t_\phi(r-r_1)$						
	c_0	c_1	c_2	c_3		
	0.36019198	−1.30766412	−7.32728884	27.19997586		

TABLE III. Electronic tight-binding parameters for the interaction between two H atoms bonded to C atoms. Parameters were obtained from fits to density functional calculations of two methane molecules, whose H atoms are separated by a distance r. The scaling function refers to Eq. (3) in the text and is a function of the separation between the two H atoms. The polynomial tail ensures that the parameters and their first derivatives go smoothly to zero between r_1 and r_{cut}.

Two-center parameter and scaling function parameters						
$V_{ss\sigma}^{H\text{-}H}$	n	n_c	r_0	r_c	r_1	r_{cut}
−0.440728	0.44949	1.56495	2.13933	0.710328	1.10	1.22
Polynomial tail $t_s(r - r_1)$						
	c_0	c_1	c_2	c_3		
	6.90045801	−11.56839584	−1244.78882144	7183.28039315		

tronic states on the surface atoms are convergent with respect to the thickness of the slab. In general, the bare surface slabs required more layers than the hydrogenated surfaces. The electronic energies are calculated from an integration of the band structure using the Pack-Monkhorst[40] scheme for determining the $\vec{k}$ point mesh in the irreducible Brillouin zone. The number of points is chosen to give a convergence better than 0.1 meV in the total band structure energy. We believe this is consistent with the accuracy of the parameters and additional convergence would be unnecessary. For the instances where the surfaces are metallic, the occupation of states is smeared using a Fermi-Dirac distribution. An advantage of this is that it allows for an analytical determination of the derivative of the Fermi level with respect to the coordinates of the atoms. Values of these convergence parameters are quoted separately below for each case.

Relaxations of the surfaces are done by the method of steepest descent, retaining the inversion symmetry throughout the relaxation. For each slab, the energy is first minimized with respect to the lattice constants to remove any additional strain due to the finite size of the slab. In all cases, this adjustment was smaller than the accuracy used in reporting our results. The forces are calculated directly by analytical expressions without any approximation, avoiding the computationally expensive task of finite differencing. The Hellmann-Feynman theorem is applied to the derivative of the band structure energy. The Hamiltonian is parametrized in terms of the two-center approximation[23] so that it is straightforward to obtain the derivative with respect to any of the coordinates. The Hubbard-like charge term is a function of the occupied wave functions of the Hamiltonian, and by employing degenerate first-order perturbation theory, we can calculate the derivatives of the wave functions with respect to the atoms coordinates. Unfortunately, since the matrix elements require cross terms between occupied and unoccupied states, the derivative of the Hubbard term is the most costly force to compute, but still is faster than a finite differencing of the energies, even on a scalar machine. The slowest operation is the diagonalization of the Hamiltonian. All of our calculations were performed on IBM RISC stations.

A. C(111) surface

The C(111) surface is the most thoroughly examined diamond surface. This surface will undergo reconstruction from (1×1) to (2×1) symmetry at temperatures exceeding $\sim 1000\,^{\circ}$C.[3,7,6,41] This reconstruction is preceded by the desorption of H and has been studied with both semiempirical[15,42,19] and first-principles methods.[11,12,43,44] In addition to adding more insight into the physics on the C(111) surface, our purpose for repeating these calculations with our tight-binding method is to give an indication of the reliability of the application of the tight-binding parameters to surfaces and H bonds on the surface.

The surface atoms on the bulk-terminated C(111) surface, shown in Fig. 2, are threefold coordinated with a dangling bond pointing normal to the plane of the surface. The atoms at the surface form a two-dimensional hexagonal lattice with one surface atom per unit cell. Since we will be examining the (2×1) reconstruction, we have used two atoms/layer in our calculation so that the unit cell is a rectangular lattice. The dangling bonds on the bulk-terminated surface form states in the gap. These states should be relatively localized, but could still interact and split into bonding and antibonding states. The band structure for the bulk-terminated C(111) surface is shown in Fig. 3. The $\overline{J}$ symmetry point is one-half of the longer reciprocal lattice vector and the $\overline{K}$ point is at the corner of the rectangular Brillouin zone. We can

TABLE IV. Repulsive parameters for the interaction between two H atoms bonded to C atoms as described in Table III and in the text.

Parameters for $\phi(r)$						
ϕ_0	m	m_c	d_0	d_c	d_1	d_{cut}
0.0546	1.02	0.8458	2.301	0.3561	1.06	1.22
Polynomial tail $t_\phi(r - r_1)$						
	c_0	c_1	c_2	c_3		
	1.29651641	−3.90234433	−103.156212802	480.62932848		

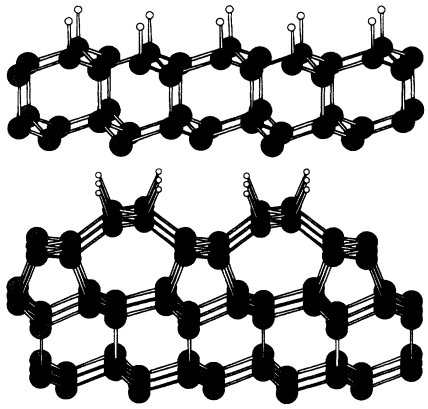

FIG. 2. Diagram of the hydrogenated ideal (top) and relaxed π reconstructed (2×1) C(111) surfaces. The surface C atoms are modeled as black balls and the hydrogen atoms are white.

see at the $\bar{\Gamma}$ point that the states do split into occupied and unoccupied states. Our occupied level is ~ 2.2 eV above the valence band, with a splitting between levels of ~ 0.75 eV. This is in quite satisfactory agreement with the local orbital *ab initio* calculations of Vanderbilt and Louie[11] who found a dangling bond state ~ 2 eV above the valence band at the $\bar{\Gamma}$ point, but with much smaller splitting between the occupied and unoccupied levels.

The dangling bond surface states are half filled, and the dispersion results in a metallic band structure. The small bandwidth (0.75 eV) suggests a possibility of important correlation effects, which could make these states (and therefore the surface) insulating. A spin-density-wave instability is another possibility. We are not aware of any experimental data on this point. Our method is, however, intended only to model local density results, and thus such correlation effects are beyond the scope of this study.

We relaxed six surface layers of a 24-layer, bulk-terminated, C(111) slab with two atoms per layer. Since the bulk-terminated surface is metallic, we used a Fermi-Dirac occupation of states with a kT width of 0.075 eV and 30 $\vec{k}$ points. In addition to the 48-atom unit cell, we also relaxed four layers of a 12-layer, 24-atom cell in order to make more direct comparisons with the size of the slabs used in the *ab initio* studies.[11,12,43] We found in our calculations that a 12-layer slab was not sufficiently thick to prohibit splittings between the surface states at the top and bottom of the slab. To avoid this problem Iarlori *et al.*[12] and Stumpf and Marcus[43] attached H to the bottom of their eight- and ten-layer slabs respectively in their plane-wave calculations. Vanderbilt and Louie used a ten-layer slab, but did not report any splitting of surface states arising from interactions between the surfaces. Upon relaxation, the bulk-terminated surface did not spontaneously reconstruct to a (2×1) surface. This is consistent with the ESD-TOF LEED data, which showed that continued annealing, even after H desorption, is required for reconstruction.[6] Our 12-layer cell lowered its energy by 0.2 eV per surface atom, mostly by decreasing the bond length between the first two layers, Δb_{12}, by 1.9%. This is similar to the results of the *ab initio* calculations of Vanderbilt and Louie who found a decrease of energy by 0.37 eV and a Δb_{12} of -3.1%.[11] Stumpf and Marcus did not cite their energy differences for their plane-wave calculation, but reported a relaxed, (1×1) bulk-terminated structure with an even bigger decrease in Δb_{12} of 4.0%.[43] Using a thicker unit cell with two more layers allowed to relax, we also found a more substantial decrease in energy of 0.39 eV per surface atom and a bigger decrease for Δb_{12} of 5.4%. The band structure for the relaxed (1×1) C(111) surface (not shown) resembles the ideal, bulk-terminated, band structure except the splitting between the unoccupied and occupied gap states at the zone center has been reduced to ~ 0.25 eV.

Pandey[42] has suggested that the C(111) surface (2×1) reconstruction is comprised of π bonded chains in the first two surface layers. This structure is similar to the one shown in Fig. 2. The zigzag chains on the top layer have bond lengths comparable to graphite. By bringing the dangling bonds closer together, the splitting between the occupied and unoccupied gap states increases, thereby lowering the electronic energy. The cost of bringing the atoms closer together on the surface is an increase in the repulsive energy between the ions. We altered the geome-

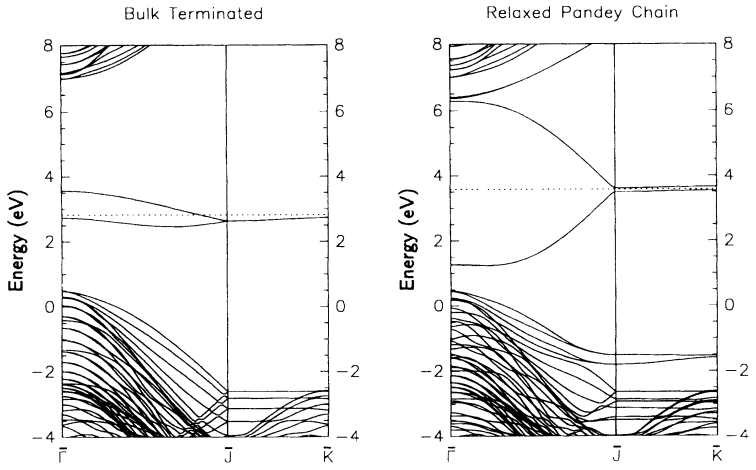

FIG. 3. Band structure of the bare C(111) bulk-terminated and relaxed π chain surfaces. The dotted line is the Fermi level. The top of the valence band is at ~ 0.45 eV.

try of the top two layers in our 24-layer bulk-terminated slab so that it would have the (2 × 1) geometry of the Pandey chain structure.[42] Our "ideal" (2 × 1) structure has surface chains with graphitic bond lengths of 1.42 Å and no dimerization. All other bond lengths are equal to the bulk diamond value of 1.54 Å. This structure required 45 $\vec{k}$ points.

The results for the relaxation of this slab are given in Table V, along with the results of the *ab initio* calculations using either plane waves[12] or localized orbitals.[11] All the calculations listed in the table report that the Pandey π reconstruction has a lower energy than the bulk-terminated surface. Our calculation indicates a favorable energy decrease even for the "ideal" π surface. The fully relaxed structure 12-layer slab was very close in energy and structure to the results of Vanderbilt and Louie. Even larger decreases ($\sim$ 50%) in energy per atom were realized when we used a thicker slab and allowed more layers to relax, indicating that the *ab initio* results may have used slabs that were still too thin.

A comparison of our band structure, in Fig. 3, for the relaxed (2 × 1) surfaces with the band structures determined by the *ab initio* calculations[11,12] (not shown) indicates very good agreement for the dispersive behavior of the gap states. At the $\bar{\Gamma}$ point, there is a large splitting of $\sim$ 5 eV between the occupied and unoccupied states. Vanderbilt and Louie showed a splitting of $\sim$ 4.8 eV and Iarlori *et al.* had a splitting of $\sim$ 3 eV. The surface gap state in both these calculations coincides with the valence band maximum at the zone center, but our tight-binding parametrization puts the surface state $\sim$ 0.5 eV above the valence band. Vanderbilt and Louie also found an additional gap state below the conduction band, just above the unoccupied dangling bond state, as did we. At the zone edge in the $\bar{J}$ direction, which is along the surface chains, the surface states become degenerate. Indeed, any dimerization of the chain will break this degeneracy. Both our calculation and that of Iarlori *et al.* had a flat band in the $\bar{J}$-$\bar{K}$ direction so that our surface chains could slightly dimerize, just enough to break the degeneracy of the $\bar{J}$-$\bar{K}$ band and make the surface nonmetallic. Vanderbilt and Louie calculated a much more dispersive band increasing in energy along the $\bar{J}$-$\bar{K}$ direction. In their case, the only way to gain band structure energy through a splitting between levels would be to force a large enough dimerization to overcome the dispersion in the $\bar{J}$-$\bar{K}$ direction. The cost in the repulsive energy to do this would be too great. More *ab initio* band structure calculations must be performed in order to confirm the dispersive behavior along this direction.

The addition of H to the C(111) surface stabilizes the surface by removing the dangling bond states from the gap, and thereby preventing reconstruction. An important aspect of growing diamond films in a H atmosphere is widely believed to be the prevention of the surface reconstruction. The H bond on the C(111) surface has been studied with *ab initio* methods by Stumpf and Marcus[43] and Zhu and Louie,[44] who were particularly interested in the anharmonicity of the H-C stretch mode. The results of these studies provide a good benchmark to evaluate our C-H parameters. We relaxed the five top layers of an 18-layer C slab with two atoms in each layer and H atoms (also relaxed) attached to the surface dangling bonds. The final coordinates of this structure are in excellent agreement with the *ab initio* results for both the geometry and energies of the H bond. We found a C-H bond length of 1.125 Å compared with the *ab initio* values of 1.12 Å from Zhu and Louie[44] and 1.1255 Å from Stumpf and Marcus.[43] In addition, we find an inward relaxation of the surface C of 0.023 Å, consistent with the results of Zhu and Louie and Stumpf and Marcus.

As a more rigorous test of the scaling of our H parameters with bond distance, we use Zhu and Louie's results for the binding energy of a surface H atom displaced a distance z from the surface. They found their binding energy fit "essentially exactly"[44] to a fourth-order polynomial:

$$V(z)\ (\text{eV}) = V_0 + 14.326z^2 - 28.422z^3 + 27.415z^4. \quad (9)$$

We repeated this calculation using our C-H parameters and plot the results in Fig 4 along with Eq. 9. Not only are we able to reproduce the anharmonicity of the C-H bond, but the agreement of the binding energy to within

TABLE V. Comparison of the tight-binding results for the relaxed π chain structure on the C(111) surface with *ab initio* calculations using plane waves and local orbitals. Energy differences are given with respect to the bulk-terminated surface. ΔE_{ideal} is the ideal Pandey chain structure defined in the text. $\bar{r}_{\text{C-C}}$ is the average bond distance in the surface chain and the percentage in parentheses is the degree of dimerization defined as $(r_1 - r_2)/(r_1 + r_2)$, where r_1 and r_2 are nearest-neighbor bond lengths. Δr_{23} is the change in bond length between the second and third layers.

	ab initio		Tight binding	
	Plane wave[a]	Local orbitals[b]	Our work	
Atomic layers	8	10	12	24
ΔE_{ideal} (eV)		−0.05	−0.44	−0.44
ΔE (eV)		−0.68	−0.70	−1.08
$\bar{r}_{\text{C-C}}$ (Å)	1.44 (1.4%)	1.47 (0.0%)	1.48 (0.2%)	1.44 (0.6%)
Δr_{23}	+8%	+8%	+6%	+9%

[a]Reference 12.
[b]Reference 11.

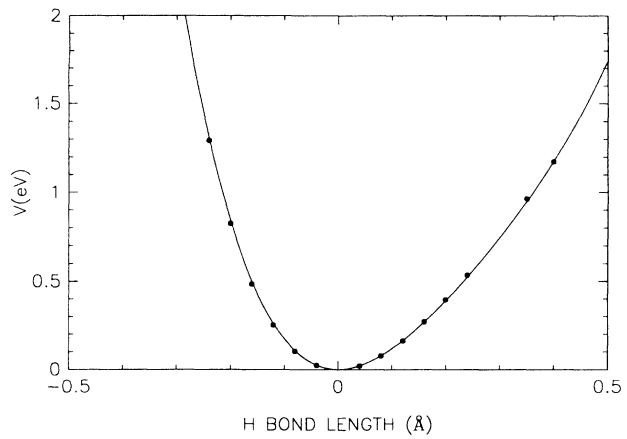

FIG. 4. Binding energy of H on the C(111) surface. The solid line is fourth-order polynomial fit to Zhu and Louie's (Ref. 44) *ab initio* calculation as described in the text. The solid points are the binding energies calculated using our tight-binding C-H parameters.

4% of the calculated local density approximation (LDA) value over a range of bond lengths $\sim \pm 35\%$ away from equilibrium indicates that the scaling of the C-H bond with distance is accurate as compared to LDA calculations.

One way to probe the H bonding environment is to measure the vibrations on the surface. We calculated the vibration modes at the zone center from a diagonalization of the full dynamical matrix of our relaxed, hydrogenated 18-layer C slab. The frequencies of the H modes are given in Table VI along with the high-resolution EELS results of Lee and Apai,[41] who examined the H modes to determine which (if any) hydrocarbons were bonded to the surface. They deconvoluted the data into H vibrations at 2850, 2930, 3000, and 3070 cm^{-1}. Infrared experiments[7] have identified a H stretch mode on the surface at $\sim$ 2830 cm^{-1}, while Zhu and Louie[44] calculated a similar but somewhat lower frequency of 2760 cm^{-1}. Lee and Apai attributed their range of frequencies to stretch modes from one or more H atoms attached to a single site containing an sp^3 or sp^2 bonded C on the (111) surface. Our unit cell consists of two monohydride bonds, and we identified H stretch modes at 2849 cm^{-1}. From an inspection of the eigenfunctions, we find these modes are very localized to each bond, with no significant coupling between neighboring H atoms. Therefore, any detectable splitting of the H stretch mode would most likely arise from the coupling of H atoms attached to the same C atom.

TABLE VI. Experimental and calculated frequencies for H modes on a fully covered C(111) surface. The phase refers to the motion of the two H bonds at the zone center of the unit cell. An out-of-phase mode would be at the zone edge of a one-H-atom cell. Identification of the modes is from the eigenfunctions of the dynamical matrix unless otherwise noted. Lee and Apai identify their high-resolution HR frequencies with vibrations from H both on the surface and on hydrocarbons attached to the surface (see Ref. 41 for full details).

HREEL frequency (cm^{-1})	Tight-binding frequency (cm^{-1})	Mode
2930		hydrocarbon stretch[a]
2850	2849	stretch
1445		hydrocarbon bend[a]
1330	1370	bend (out of phase)
	1112	bend (in phase)
1060	1084	bend (in phase)
	1045	bend (out of phase)

[a]Reference 41.

The proximate environment of the H atom on the C(111) surface has C_{3v} symmetry and if the H bend modes were highly localized, there would be two degenerate modes for each C-H bond. Instead, unlike the H stretch mode, the bend modes are not localized and couple strongly to the phonons of the lattice. We list the H bend frequencies in Table VI to illustrate this point. In addition to the coupling with the bulk phonons, there is also an interaction between neighboring C-H bend modes, which we assign as out of phase and in phase, relative to the motion of the H atoms. For comparison, we have also listed the deconvoluted EELS frequencies of Lee and Apai,[41] who assigned their modes to vibrations of H atoms on hydrocarbons attached to the surface by comparing to known molecular frequencies and trends. Hamza *et al.*[6] argued that the H bend frequencies, observed near 1290 cm^{-1},[5] most likely arise from monohydride bonds on the surface, based on their angular resolved ESD data, but conceded that their ESD data were not definitive. Even though our frequencies for the H bend modes on the surface seem to coincide with the EELS data in Table VI, they probably are not as reliable as the stretching frequencies for two reasons: 1) Our parameters were obtained explicitly from bond stretching distortions (rather than bending) of the methane molecule, and (2) the error in the highest-frequency bulk phonon calculated with these C parameters is $\sim$ 5%,[21] but the surface phonon frequency, which couples to the H bend modes, could be less accurate. The information gained from these results overall is that the bend modes couple with the lattice phonons, splitting over a range of $\sim$ 300 cm^{-1}, and that the identification of frequencies in this range to vibrations of specific hydrocarbons by comparison to the relative vibrations of the hydrocarbon molecule may be difficult. The localized stretching mode should provide a better indication of the H bonding environment on the surface.

By combining their infrared (ir) and LEED data, Chin *et al.*[7] have been able to observe the H stretch vibration as the C(111) surface undergoes (2 × 1) reconstruction. They found that dosing the (2 × 1) surface forced a reconstruction back to (1 × 1), mediated by a metastable H bonded state. We added H to our relaxed π reconstructed surface and found a stable (2 × 1) structure shown in Fig. 2. This structure resembles the top two surface layers of the hydrogenated C(110) surface discussed in Sec. III C. H attaches to each of the atoms in the surface chain. The C-H bond length is 1.128 Å and the chain bond lengths are stretched to 1.562 Å with

0.3% dimerization. All the bond lengths in the first two layers have stretched by ~ 0.01 Å. The bond lengths between the second and third layers, Δr_{23}, have increased by 3% from the ideal bulk value, compared with the relaxed bare π surface, whose bond lengths increased by 9%. Chin *et al.*[7] tracked a H stretching frequency at 2860 cm^{-1} [30 cm^{-1} higher than the one measured on the (1×1) surface] that appeared when the (2×1) bare surface was dosed with H. This peak disappeared when the surface was fully annealed back to a (1×1) structure, but the peak at 2830 cm^{-1} remained. We did not calculate the H stretch frequency of this structure but we did find that the H stretch mode on a similar C(110) surface, discussed in Sec. III C, was 14 cm^{-1} higher than on the C(111) (1×1) surface, indicating that it is possible that the structure in Fig. 2 is the metastable structure Chin *et al.* observed. The energy of this surface is ~ 0.65 eV per surface C higher than the relaxed, hydrogenated (1×1) surface. This implies that the surface will go to the more favorable (1×1) symmetry, but must first overcome an energy barrier, and that H alone is not solely responsible for the reconstruction. Since Chin *et al.*[7] observed the (2×1) to (1×1) reconstruction under conditions of partial H coverage, it is possible that the true mechanism for reconstruction involves partially hydrogenated chains rather than fully hydrogenated chains.

B. C(100) surface

Unlike the C(111) and C(110) surfaces, the C(100) surface has two dangling bonds on each atom. Since they are located at the same site and are not orthogonal, they should mix and split into two distinct gap levels centered near the Fermi energy. Shown in Fig. 5 is the band structure for the bare C(100) surface calculated with two surface atoms per unit cell. This surface is not metallic since the occupied bands are completely full. At the $\bar{\Gamma}$ point we can see four distinct surface states from the four unsatisfied surface bonds. Along the $\bar{J}$ direction, which is along the direction of the dangling bonds, the levels become doubly degenerate. This indicates that the ~ 1 eV splitting of states around the Fermi level is due to the mixing of the on-site dangling bonds and that the off-site interactions separated by a distance of ~ 2.5 Å account for the small splitting, most visible at the zone center. This is in qualitative agreement with Lowther's[36] and Ciraci and Batra's[45] tight-binding results for the bare surface, except for the notable exception that Ciraci and Batra's antibonding surface state barely crosses the Fermi level at the diagonal zone edge, so their surface would be metallic. The crossing of this state along thia direction (not shown in our figure) did not occur in our calculation, but could still be correct since Ciraci and Batra used a more detailed, self-consistent method to calculate the band structure, which included nonorthogonal orbitals.[45] Gavrilenko's[35] tight-binding calculation shows only one occupied state located at the center of the gap. This means that the two dangling bonds at each site either: (1) do not mix and are degenerate or (2) mix sufficiently to push the unoccupied state into the conduction band. We believe the latter reason is the explanation of his result, which is therefore a function of his electronic parameters, which included an extra s^* state. This s^* state would add more s character to the dangling bonds, allowing more mixing between the states and increasing the splitting of the levels.

The fact that the two levels arise from the splitting of the on-site dangling bonds rather than between neighboring dangling bonds means that an energy gain in forming surface dimers is not a Peierls type of distortion as it was in the case of the (2×1) C(111) surface, but occurs because one of the dangling bonds on each atom is eliminated. Figure 5 shows the electronic structure of the (2×1) reconstructed surface. There are now only two states remaining in the gap, corresponding to the dangling bonds on each of the two surface atoms in the unit cell. These states are split by 2.7 eV and show very little dispersion. As in the bare (1×1) surface, our results differ from Gavrilenko's in that he calculates only one (occupied) surface level in the gap. Again, we believe this difference is due to the additional s character of the dangling bonds in his calculations. *Ab initio* pseudopotential calculations of Yang *et al.*[14] show a density

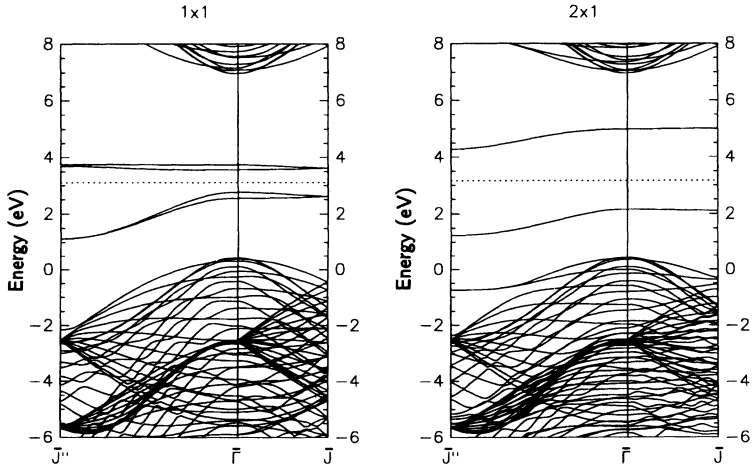

FIG. 5. Band structure of the bare C(100) surfaces. The dotted line is the Fermi level. The top of the valence band is at ~ 0.45 eV.

of states which has both occupied and unoccupied gap states near the valence band, more consistent with our results.

The coordinates used for all the C(100) band structures have been obtained by relaxing six layers of the 24-layer unit cell, with two C atoms per layer. The (2×1) surface was found to be 1.86 eV per surface atom lower in energy than the ideal, bulk-terminated (1×1) structure. For the relaxed (1×1) symmetry, we could only allow atom displacements along the normal to the surface, otherwise the surface would reconstruct. The relaxed coordinates of the (1×1) and (2×1) bare C(100) surfaces are given in Table VII along with the *ab initio* results of Yang *et al.*[14] for comparison. The relaxed (2×1) surface shows a large decrease in spacing between the first and second layers that is in excellent agreement with the *ab initio* results. In the remaining layers the trends are the same, but the magnitudes differ somewhat. Part of the reason for this discrepancy is that the *ab initio* calculation used smaller unit cells of 12 C layers, terminated by H on the bottom, and allowed all the layers to relax except the bottom C layer.

Other than reconstructing to a (2×1) surface, the dangling bond states of the (1×1) surface can be removed by the addition of H, which will stabilize the (1×1) surface. It has been observed that heating the H-covered C(100) surface to temperatures greater than 1300 K will force the (1×1) surface to undergo a (2×1) reconstruction.[8] The structure of the hydrogenated surface has been studied with a variety of techniques ranging from empirical classical potentials[15,46] to *ab initio* pseudopotential methods,[14] but the results are not conclusive for the final geometries or band structures. Starting with the fully relaxed hydrogenated (1×1) surface, we removed one H atom at a time and re-relaxed the structures in order to generate the configurations corresponding to the four surfaces [H_x:C(100), x = 2, 1.5, 1, and 0.5] diagrammed in Fig. 6 .

Table VIII lists the final relaxed geometries for all the structures shown in Fig. 6. The hydrogenated (1×1) surface has two H atoms attached to each surface C and is therefore referred to as the dihydride surface. If one assumes H bond lengths comparable to those found on the C(111) surface and ideal tetrahedral bond angles, then the H atoms on neighboring surface carbon atoms would only be ~ 0.7 Å apart. These H atoms would strongly repel each other, and having the capability of dealing with such -H:H- interactions is the reason for obtaining the interaction parameters between nonbonded H atoms as described in Sec. II. Due to this repulsion between the H atoms, the dihydride surface has a contracted C-H bond length and H bonds bent towards the surface normal by 18° from the ideal tetrahedral direction, so that the neighboring H atoms are now 1.30 Å apart. There has been disagreement in the literature as to whether this structure is actually the (1×1) structure observed by LEED. Empirical[46] and *ab initio*[14] results have found that this dihydride phase is unstable, though Zheng and Smith, using a slab MNDO method,[20] found a stable surface with a *stretched* C-H bond of 1.13 Å and a bond angle to the surface normal of 35.4°. DF cluster calculations resembling a fluorinated C(100) surface also found the (1×1) difluoride structure to be unstable.[47] Other empirical and semiempirical studies[17,35] have found stable dihydride structures with *contracted* bond lengths of less than 1.10 Å as did we. We systematically twisted the H bonds out of the plane defined by the ideal positions of the dihydride bond, and allowed the remainder of the lattice to relax. The direction, but not the length, of the H bonds was held constant. We found that the energy will increase as the twist angle increases, in agreement with the calculations of Zheng and Smith.[20]

Removal of one of the H atoms from the dihydride surface leaves three H atoms for every two surface C atoms, and we refer to this surface as a 3/2 hydride. After relaxation, the odd H atom is located midway between the two surface carbons as seen in Fig. 6 (x = 1.5). This surface

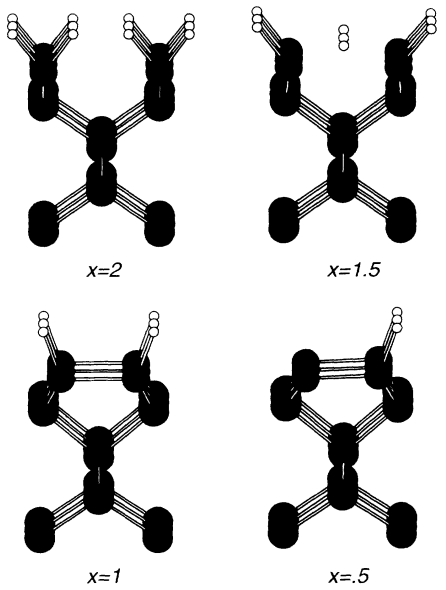

FIG. 6. Side view of the final relaxed C(100) surfaces with different hydrogen coverage H_x:C(100), where x=2, 1.5, 1, and 0.5. The surface C atoms are modeled as black balls and the hydrogen atoms are white. The dihydride surface (x=2) is the first one shown and the monohydride (x = 1) is the third one shown.

TABLE VII. Relaxed geometry for bare C(100) surfaces. $r_{C\text{-}C}$ is the surface dimer bond length. The atoms in the (1×1) calculation were held in their (1×1) symmetry. Δd_{ij} is the change in spacing between the ith and jth layers as compared to the ideal bulk-terminated structure. *Ab initio* calculations, taken from Ref. 14, are given for comparison.

	Tight binding		*ab initio*[a]
	1×1	2×1	2×1
$r_{C\text{-}C}$ Å	2.511	1.398	1.40
Δd_{12} (%)	+0.36	−24.8	−24
Δd_{23} (%)	+2.88	+8.26	+3
Δd_{34} (%)	−0.72	−1.15	−0.6
Δd_{45} (%)	~ 0.0	−0.74	

[a]Reference 41.

TABLE VIII. Relaxed geometry for the H_x:C(100) surfaces, which correspond to the configurations shown in Fig. 6. See Table VII for explanation of some of the parameters. $\theta_{\text{H-C-}\hat{n}}$ is the angle between the H bond and the normal to the surface. The value in parentheses for the H bond on the 3/2 hydride surface refer to the shared H atom. *ab initio* calculations are taken from Ref. 14 and are given for comparison.

	Tight-binding				*ab initio*[a]
	Dihydride	3/2 hydride	Monohydride	1/2 hydride	Monohydride
	$x = 2$	$x = 1.5$	$x = 1$	$x = 0.5$	$x = 1$
$r_{\text{C-C}}$ (Å)	2.51	2.36	1.617	1.58	1.67
$r_{\text{C-H}}$ (Å)	1.07	1.12 (1.27)	1.122	1.126	1.17
$\theta_{\text{H-C-}\hat{n}}$	37.3°	32.9°(56.2°)	20.2°	17.8°	23.9°
Δd_{12} (%)	−4.95	−5.41	−9.24	−15.48	−3
Δd_{23} (%)	+0.23	+ 2.81	+12.71	+4.04	−0.3
Δd_{34} (%)	−1.01	−0.91	−5.47	−0.71	
Δd_{45} (%)	−0.13	+0.70	−5.17	+0.46	

[a]Reference 14.

has reconstructed to (2×1), but the surface bond has only contracted by ∼0.15 Å compared with ∼ 0.9 Å for the fully reconstructed (2 × 1) monohydride surface. These C atoms are 2.36 Å apart, in the region of the polynomial tail cutoff for the C parameters, where the increase in bonding is changing rapidly and may be responsible for the resulting slight dimerization. The shared H atom is 1.27 Å away from both surface carbons, only ∼ 14% farther than the singly bonded H atom, which is 1.12 Å, away. By removing the odd H atom, we obtain the monohydride surface. The relaxed (2×1) monohydride surface has a C atom dimer that has contracted 35% from the (1 × 1) bond length. Table VIII compares the results of these structures including the *ab initio* results[14] for the monohydride surface for comparison. There are slight differences between the methods, but again the general trends are the same. Though our results are consistent with those of Zheng and Smith,[20] who found a −15% change in spacing between the first two layers, our spacing is still much larger than reported from the *ab initio* calculation.[14]

Photoemission data taken by Hamza *et al.*[8] indicate that the hydrogenated (1 × 1) surface has no occupied gap states, consistent with our band structure in Fig. 7 of the dihydride surface. The addition of H to the surface should remove the dangling bond states from the gap. The contraction of the H bonds pushes the H antibonding states below the conduction band, but since our parameters were optimized for describing the occupied states, we cannot rule out the possibility that this band may still actually lie in resonance with the conduction band. From his tight-binding calculation, Gavrilenko[35] found no occupied states in the gap, but Lowther[36] did find occupied states, inconsistent with the photoemission data. As a candidate for the (1 × 1) H-covered surface, the 3/2 hydride surface fails because the surface is slightly dimerized and there is a half-filled state in the gap.

For the (2 × 1) reconstructed surface, photoemission data indicated that there were occupied states in the gap.[8] Our band structure in Fig. 7 shows no gap states for the monohydride surface, in agreement with the *ab initio* results.[14] The clear implication is that the observed (2 × 1) reconstructed surface is not the simple monohydride phase. Gavrilenko,[35] however, did find occupied states in the gap for the monohydride surface and concluded that the (2 × 1) surface was a fully hydrogenated monohydride surface. Experimentally, Hamza *et al.*[8] found that the (2 × 1) surface reconstruction was accompanied by the desorption of H. Two distinct velocity distributions of the desorbed H were observed. The higher velocity preceded (2 × 1) reconstruction while the lower velocity desorption continued after the surface reconstructed. We suggest that the slower desorption is from the breaking of the monohydride bond and that the (2 × 1) surface is partially (rather than fully) covered with H, so that the half-hydride surface would probably be more representative of the actual H coverage. More recently, Lee and Apai[41] found from their EELS measurement of the H vibration modes that there was no H remaining on the annealed C(100) surface, and attributed Hamza *et al.*'s results to the desorption of bulk H that had diffused to the surface. The band structure of the bare (2×1) surface, shown in Fig. 5, has an occupied and an unoccupied surface state, split by ∼ 3 eV at the zone center. The band structure of our half-hydride configuration, shown in Fig. 7, has a partially filled gap state, which would be more consistent with the photoemission data,[8] which found no unoccupied states between 1.17 and 5.5 eV above the Fermi level.

C. C(110) surface

The C(110) surface, shown in Fig. 8, consists of layers of zigzag chains, stacked alternately. Within each layer, the C chains are relatively far apart, separated by 2.9 Å. The bulk-terminated, threefold coordinated, surface atoms have dangling bonds pointing 19.5° away from the surface normal. We found the surface states on the bulk-terminated C(110) surface to be more confined than those on the C(100) and C(111) surface, so only 18 C layers were required to prevent coupling of surface states on the top and bottom of the slab. We allowed the top six layers to relax, which was more than necessary since the sixth layer was stable in its bulk configuration. Due to the dispersive nature of the surface states on the bare surface,

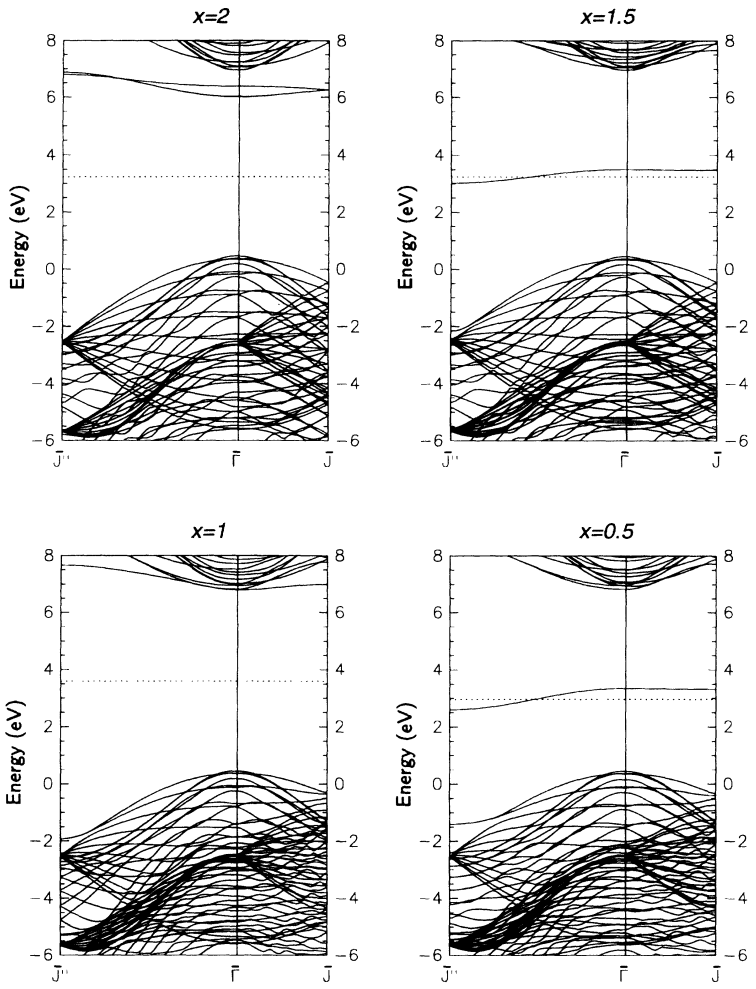

FIG. 7. Band structure of the H_x:C(100) surfaces as shown in Fig. 6. The dotted line is the Fermi level. The top of the valence band is at ~ 0.45 eV.

we needed 40 $\vec{k}$ points, but for the fully hydrogenated surface, only 20 $\vec{k}$ points were required. In Table IX we give the results for the final relaxed structures for the bare and hydrogenated C(110) surfaces. The percentage in parentheses next to the bond lengths is the degree of dimerization.

Lurie and Wilson[2] observed that the bare C(110) surface does not reconstruct. We also find that the (1×1) surface does not undergo (2×1) reconstruction. The two surface atoms in the (1×1) unit cell have a dangling bond, so we expect two states in the gap. These dangling bonds are only a bond length apart and should interact and split into bonding and antibonding levels. In the direction across the chains, corresponding to $\bar{\Gamma}$-$\bar{J}'$, these levels are nondegenerate, but along the zigzag chains ($\bar{\Gamma}$-$\bar{J}$) the antibonding and bonding levels become degenerate at the zone edge. Dimerization of the surface C atoms will break this degeneracy and lower the electronic energy. This can be seen in the band structures for the bulk-terminated and relaxed, bare C(110) surfaces in Fig. 9. The chain bond lengths on the relaxed bare surface are contracted to 1.43 Å, and have slightly dimerized; just enough to break the degeneracy at the zone edge. The bulk-terminated C(110) surface lowers its energy by 0.38 eV per surface atom by moving the surface atoms inward by 0.15 Å and by partially "straightening" the zigzag chain on the surface. This brings the dangling bonds closer together, thereby lowering the level of the occupied gap state.

Photoemission data indicate that the gap state on the bare C(110) surface disappears with the addition of H and reappears when H is again removed.[9] Table IX shows that the addition of H atoms to the surface prevents the contraction of the surface C bonds and reduces the change in spacing between layers. The hydrogenated sur-

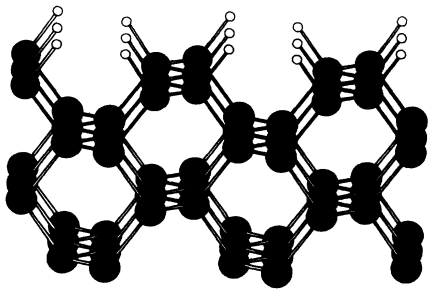

FIG. 8. Diagram of the fully hydrogenated C(110) surface. The hydrogen atoms are white and surface C atoms are black.

TABLE IX. Relaxed geometries for the bare and hydrogenated C(110) surfaces. $\bar{r}^{(i)}_{\text{C-C}}$ is the average bond length in the zigzag plane in the ith layer. The value in parentheses is the degree of dimerization in the zigzag chains defined as $(r_1-r_2)/(r_1+r_2)$, where r_1 and r_2 are nearest-neighbor bond lengths. $\theta_{\text{H-C-}\hat{n}}$ is the angle between the H bond and the normal to the surface.

		H coverage	
	Bare	Half hydride	Fully hydrogenated
$r_{\text{C-H}}$ (Å)		1.126	1.124
$\theta_{\text{H-C-}\hat{n}}$		21.4°	18.3°
$\bar{r}^{(1)}_{\text{C-C}}$ (Å)	1.43 (0.8%)	1.48 (0.2%)	1.52 (0.3%)
Δd_{12} (%)	−14.8	−3.3	−1.4
$\bar{r}^{(2)}_{\text{C-C}}$ (Å)	1.49 (0.7%)	1.53 (0.4%)	1.53 (0.5%)
Δd_{23} (%)	2.5	0.84	−0.1
$\bar{r}^{(3)}_{\text{C-C}}$ (Å)	1.53 (0.5%)	1.54 (0.5%)	1.54 (0.6%)
Δd_{34} (%)	−0.4	−0.02	0.08
$\bar{r}^{(4)}_{\text{C-C}}$ (Å)	1.54 (0.6%)	1.54 (0.6%)	1.54 (0.3%)
Δd_{45} (%)	0.2	0.09	0.01
$\bar{r}^{(5)}_{\text{C-C}}$ (Å)	1.54 (0.6%)	1.54 (0.6%)	1.54 (0.3%)

face has no gap states, but the half-hydrogenated surface has one half-filled state in the gap due to the dangling bonds. Even though there are no longer any gap states, the hydrogenated surfaces are still slightly dimerized. This could be related to the result that the layers below the surface prefer to dimerize as indicated in Table IX. The half-hydride structure was the only one of the three C(110) surfaces to show any significant buckling of the chains. The C atom that has a H atom attached moved outward by 0.024 Å and the bare C atom moved inward by 0.081 Å. The H bond is also slightly longer and bent 3° further away from the normal compared to the fully hydrogenated surface.

We calculated the eigenvalues of the full dynamical matrix for the hydrogenated surface to obtain the H vibration frequencies at the zone center (see Table X). We find a splitting of both the bend and stretch H modes (there are two H atoms per surface cell). This is different from the H vibrations on the C(111) surface in that the H bonds on the C(110) are closer together and can interact more strongly. The high-frequency stretch modes are still very localized, but the bend modes couple to the lattice and are not doubly degenerate. On the C(110) surface, one bend mode is perpendicular to the plane of the zigzag chain and the other mode is parallel to the plane. The breaking of the degeneracy and the coupling of the modes widen the band so that, according to our calculation, absorption from the H bending modes can occur in the range from $\sim$ 1000 to $\sim$ 1370 cm^{-1}. The modes would not interact as strongly on a partially covered surface and the width of the H absorption bands should be thinner.

IV. CONCLUSION

By adopting Xu *et al.*'s[21] PTBF for C and adding accurate parameters for H, we have been able to do a thorough study of the energies and dynamics of H on diamond surfaces. A comparison of the geometries of the C(111) (1×1) and (2×1) π reconstructed surfaces and H surface vibrations has demonstrated that the method is in reasonable agreement with *ab initio* calculations on these surfaces. Adding H to the C(111) (2×1) reconstructed surface does not force the surface to reconstruct back to (1×1), but rather, a stable surface that resembles the hy-

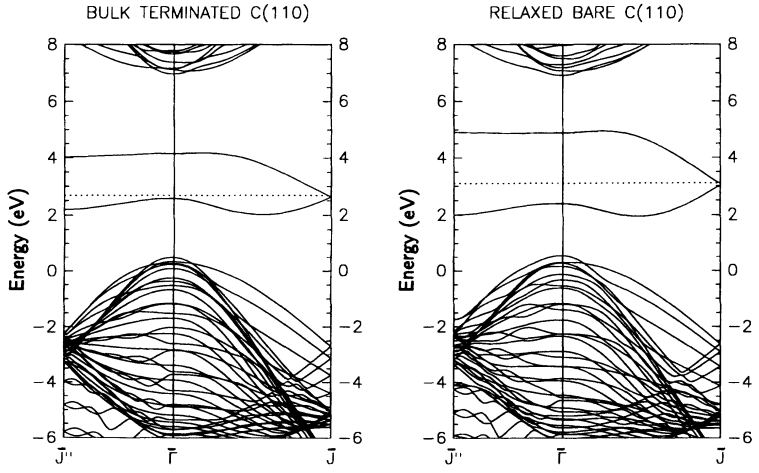

FIG. 9. Band structure of the bare C(110) surface for the bulk-terminated and relaxed structures. The dotted line is the Fermi level. The top of the valence band is at $\sim$ 0.45 eV.

TABLE X. Calculated frequencies for H modes on a fully covered C(110) surface with two surface atoms in the unit cell. The phase is in reference to the motion of the two H bonds in the unit cell at the zone center. The bending modes are distinguished by vibrations parallel or perpendicular to the plane defined by the C-C chains.

Frequency (cm^{-1})	Mode
2863	stretch (in phase)
2855	stretch (out of phase)
1369	bend out of plane (out of phase)
1191	bend in plane (in phase)
1099	bend out of plane (in phase)
998	bend in plane (out of phase)

drogenated C(110) surface is formed. We have calculated the geometries of the relaxed C(100) dihydride structure and found that the repulsion of the neighboring H atoms will contract the C-H bonds. Removal of a H atom from this surface results in a 3/2 hydride surface, where the odd H is shared equally between two C surface atoms. This surface would have a partially occupied state in the gap. Removal of H from the (2×1) surface shrinks the C dimer bond to 1.62 Å for the fully covered, monohydride surface to 1.398 Å for the bare surface. We have also presented the geometries, band structures, and H vibrations for the C(110) surface. Similar to the reconstructed C(100) surface, the bare C(110) surface has bond lengths comparable to those of graphite. Examination of the band structure and relaxed geometries indicates that the bare C(110) surface should dimerize. Covering the surface with H increases the C bond lengths to $\sim$ 1.52 Å. The H stretch vibration on the C(110) surface was determined to be $\sim$ 14 cm^{-1} higher than on the C(111) surface.

These results demonstrate that PTBF techniques can still be very useful for studying large systems with many configurations. In particular, fitting the PTBF parameters explicitly over a range of bond distances provides a more reliable Hamiltonian for calculating total energies or examining surface dynamics. Even though the parameters were optimized for total energies, we presented band structure results to identify the surface states that drive the relaxations and also to aid the interpretation of photoemission data. With the addition of our H parameters, this method can be applied to studying the interaction of hydrocarbons with the surface and should also be useful in investigating large hydrocarbon clusters.

ACKNOWLEDGMENTS

The authors would like to thank Mark Pederson for the use of his DF code and Andrew Quong for his guidance in performing the DF calculations. B.N.D. acknowledges support from the National Research Council. This work was supported by Office of Naval Research Contract No. N00014-93-WX-2C023.

[1] See, for example, D. Huang, M. Frenklach, and M. Maroncelli, J. Phys. Chem. **92**, 6379 (1988); S.J. Harris, D.N. Belton, and R.J. Blint, J. Appl. Phys. **70**, 2654 (1991); D.N. Belton and S.J. Harris, J. Phys. Chem. **96**, 2371 (1992); D. Huang and M. Frenklach, *ibid.* **96**, 1868 (1992); J.E. Butler and R.L Woodin, Philos. Trans. R. Soc. London, Ser. A **342**, 209 (1993); B. Sun, X. Zhang, and Z. Lin, Phys. Rev. B **47**, 9816 (1993).
[2] P.G. Lurie and J.M. Wilson, Surf. Sci. **65**, 453 (1977).
[3] B.B. Pate, Surf. Sci. **165**, 83 (1986).
[4] B.B. Pate, M.H. Hecht, C. Binns, I. Lindau, and W.E. Spicer, J. Vac. Sci. Technol. **21**, 364 (1982).
[5] B.J. Waclawski, D.T. Pierce, N. Swanson, and R.J. Celotta, J. Vac. Sci. Technol. **21**, 368 (1982).
[6] A.V. Hamza, G.D. Kubiak, and R.H. Stulen, Surf. Sci. Lett. **206**, L833 (1988).
[7] R.P. Chin, J.Y. Huang, Y.R. Shen, T.J. Chuang, H. Seki, and M. Buck, Phys. Rev. B **45**, 1522 (1992).
[8] A.V. Hamza, G.D. Kubiak, and R.H. Stulen, Surf. Sci. **237**, 35 (1990).
[9] S.V. Pepper, J. Vac. Sci. Technol. **20**, 213 (1982).
[10] S.V. Pepper, Surf. Sci. **123**, 47 (1982).
[11] D. Vanderbilt and S.G. Louie, Phys. Rev. B **29**, 7099 (1984); *ibid.* J. Vac. Sci. Technol. B **1**, 723 (1983).
[12] S. Iarlori, G. Galli, F. Gygi, M. Parrinello, and E. Tosatti, Phys. Rev. Lett. **69**, 2947 (1992).
[13] K.A. Jackson, in *Proceedings of the 2nd International Conference on the New Diamond Science and Technology*, edited by R. Messier and J. Glass, MRS Symposia Proceedings No. 162 (Materials Research Society, Pittsburgh, 1991).
[14] S.H. Yang, D.A. Drabold, and J.B. Adams, Phys. Rev. B **48**, 5261 (1993).
[15] D.W. Brenner, Phys. Rev. B **42**, 9458 (1990).
[16] J.A. Harrison, C.T. White, R.J. Colton, and D.W. Brenner, Mater. Res. Bull. **18**, 50 (1993).
[17] W.S. Verwoerd, Surf. Sci. **108**, 153 (1981).
[18] F. Bechstedt and D. Reichardt, Surf. Sci. **202**, 83 (1988).
[19] X.M. Zheng and P.V. Smith, Surf. Sci. **261**, 394 (1992).
[20] X.M. Zheng and P.V. Smith, Surf. Sci. **256**, 1 (1991).
[21] C.H. Xu, C.Z. Wang, C.T. Chan, and K.M. Ho, J. Phys. Condens. Matter **4**, 6047 (1992).
[22] B.I. Zhang, X.Z. Wang, and K.M. Ho, Chem. Phys. Lett. **193**, 225 (1992).
[23] J.C. Slater and G.F Koster, Phys. Rev. **94**, 1498 (1954).
[24] D. Papaconstantopoulos, *Handbook of the Band Structure of Elemental Solids* (Plenum Press, New York, 1986).
[25] W.A. Harrison, *Electronic Structure and the Properties of Solids. The Physics of the Chemical Bond* (Dover, New York, 1989).
[26] D.J. Chadi, Phys. Rev. Lett. **9**, 1062 (1978).
[27] D. Tománek and M.A. Schlüter, Phys. Rev. Lett. **56**, 1055 (1986).
[28] P.B. Allen, J.Q. Broughton, and A.K. McMahan, Phys. Rev. B **34**, 859 (1986).
[29] L. Goodwin, A.J. Skinner, and D.G. Pettifor, Europhys Lett. **9**, 701 (1989).
[30] The Mulliken population analysis is obtained by summing the squares of each element of the eigenfunctions associated with the orbitals on a given atom, multiplied by the occupation of the state.
[31] C.Z. Wang and K.M. Ho, Phys. Rev. Lett. **71**, 1184 (1993).

[32] K.C. Pandey, Phys. Rev. B **14**, 1557 (1976).
[33] D.C. Allan and E.J. Mele, Phys. Rev. B **31**, 5565 (1985).
[34] B.J. Min, Y.H. Lee, X.Z. Wang, C.T. Chin, and K.M. Ho, Phys. Rev. B **46**, 9677 (1992).
[35] V.I. Gavrilenko, Phys. Rev. B **47**, 9556 (1993).
[36] J.E. Lowther, Solid State Commun. **56**, 243 (1985).
[37] Y. Wang, G.F. Bertsch, and D. Tománek, Z. Phys. D **25**, 181 (1993).
[38] M.R. Pederson and K.A. Jackson, Phys. Rev. B **41**, 7453 (1990).
[39] G. Herzberg, *Infrared and Raman Spectra of Polyatomic Molecules* (D. Van Nostrand Co., New York, 1945), and references therein.
[40] J.D. Pack and H.J. Monkhorst, Phys. Rev. B **16**, 1748 (1977).
[41] S.-Tong Lee and G. Apai, Phys. Rev. B **48**, 2684 (1993).
[42] K.C. Pandey, Phys. Rev. B **25**, 4338 (1982).
[43] R. Stumpf and P.M. Marcus, Phys. Rev. B **47**, 16 016 (1993).
[44] X. Zhu and S.G. Louie, Phys. Rev. B **45**, 3940 (1992).
[45] S. Ciraci and I.P. Batra, Phys. Rev. B **15**, 3254 (1977).
[46] Y.L. Yang and M.P. D'Evelyn, J. Vac. Sci. Technol. **10**, 978 (1992).
[47] M.R. Pederson and W.E. Pickett, in *Novel Forms of Carbon*, edited by C. L. Renschler, J. J. Pouch, and D. M. Cox, MRS Symposia Proceedings No. 270 (Materials Research Society, Pittsburgh, 1992), p. 389.

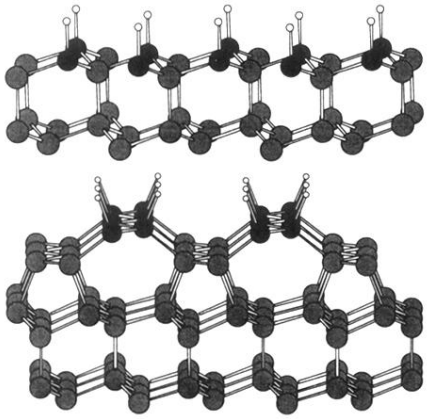

FIG. 2. Diagram of the hydrogenated ideal (top) and relaxed π reconstructed (2×1) C(111) surfaces. The surface C atoms are modeled as black balls and the hydrogen atoms are white.

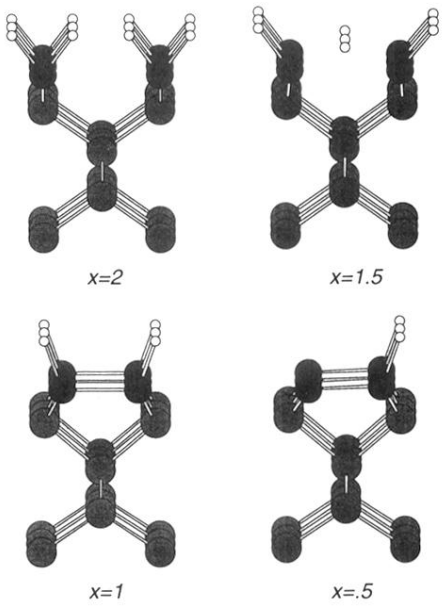

FIG. 6. Side view of the final relaxed C(100) surfaces with different hydrogen coverage H_x:C(100), where x=2, 1.5, 1, and 0.5. The surface C atoms are modeled as black balls and the hydrogen atoms are white. The dihydride surface (x=2) is the first one shown and the monohydride (x = 1) is the third one shown.

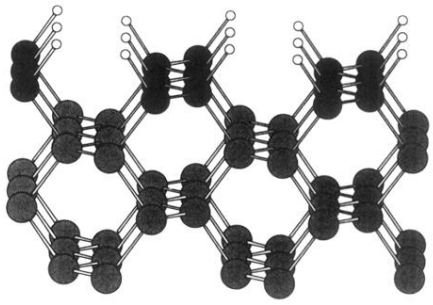

FIG. 8. Diagram of the fully hydrogenated C(110) surface. The hydrogen atoms are white and surface C atoms are black.